

# Feedback Control of a Nonlinear Dual-Oscillator Heartbeat Model

Michael E. Brandt<sup>1</sup>, Guanyu Wang<sup>1</sup>, and Hue-Teh Shih<sup>2</sup>

<sup>1</sup> Center for Computational Biomedicine & Neurosignal Analysis Laboratory,  
University of Texas Health Science Center–SHIS, Houston, TX 77030, USA

<sup>2</sup> Baylor College of Medicine, Department of Medicine, Houston, TX 77030, USA

**Abstract.** We describe a feedback control method for stabilizing some pathological behaviors of a nonlinear heartbeat model, with and without additive random noise. The controller is discretized to demonstrate how it might be implemented in a practical pacemaker design. Comparisons with some other control methods are discussed.

## 1 Introduction

In recent years, there has been much attention given to the notion of stabilization of abnormal cardiac rhythms using a nonlinear dynamical systems paradigm. This approach is characterized by the application of low-intensity electrical perturbing stimuli applied with variable timing. The first such attempt at controlling cardiac chaos can be traced back to Garfinkel *et al.* [1], who stabilized drug-induced cardiac arrhythmias in the *in vitro* rabbit ventricle by altering the timing of the interbeat cardiac intervals. It was shown that administering low-intensity electrical shocks directly to the septum at irregular intervals determined by the OGY method [2] could convert the arrhythmia to periodic beating. Despite some success using the OGY method, there remain difficulties in applying it in actual cardiac preparations. It is computationally complex and unintuitive, requiring that the locations of saddle-type UFP's be found using the method of delay-coordinate embedding (to this end a prolonged learning phase is needed). The sensitivity of the state point to changes in parameters, and the timing and the amplitude of the electrical stimulation are difficult to determine.

Another potential drawback of the OGY method is that a constant vigilance must be maintained in case the system veers away from the stable manifold of the unstable target. Several studies (e.g., [7-11]) have overcome some of these limitations by introducing a variety of discrete map models to simulate the dynamics of interbeat intervals and by demonstrating various control strategies using time-delay feedback (for a partial review see [12]). The cardiac conduction system is considered to be a network of self-excitatory pacemakers [3, 4], with the sinoatrial (SA) node having the highest intrinsic rate. Subsidiary pacemakers with slower firing frequencies are located in

---

Corresponding author (Brandt) email: mbrandt@uth.tmc.edu

the atrioventricular (AV) node and the His-Purkinje system. The SA node is the dominant pacemaker of the heart. Electrical impulses travel from it to the ventricles through the AV junction, which is traditionally regarded as a passive conduit. To take advantage of the ever-increasing knowledge of cardiac dynamics we use here a previously detailed mathematical model having a strong correspondence to the physiology of the heart's conduction system [5, 6]. The model is a two-coupled nonlinear oscillator implemented in a set of four ordinary differential equations. We propose a feedback control algorithm which uses the difference in interbeat intervals between the SA and AV nodes. A possible main utility of this method may be as a software-based approach to generating lower chamber pacing stimuli which could replace current pacemaker hardware that utilizes a reel for stimuli timing. Replacing such hardware might allow a pacemaker to become magnet-safe so that patients can undergo magnetic resonance scans without pacemaker removal or damage.

## 2 Model Description

The coupled nonlinear oscillator model studied here describes in a natural way the interaction between the SA and AV nodes. The generated waveforms of the model resemble the action potentials of cells in both these nodes. The abnormal behavior of the model corresponds well to several pathophysiological symptoms observed in the human heart as detailed in [5, 6]. We use this model to test the method of feedback control to resynchronize the AV and SA nodes when they demonstrate some pathological coupled rhythm pattern such as bigeminy or trigeminy. The continuous model relations are given by

$$\dot{x}_1 = \frac{1}{C_{SA}} x_2, \quad (1)$$

$$\dot{x}_2 = -\frac{1}{L_{SA}} [x_1 + g(x_2) + R(x_2 + x_4)], \quad (2)$$

$$\dot{x}_3 = \frac{1}{C_{AV}} x_4, \quad (3)$$

$$\dot{x}_4 = -\frac{1}{L_{AV}} [x_3 + f(x_4) + R(x_2 + x_4)], \quad (4)$$

where  $g(x) = f(x) + h(x)$ ,  $f(x) = x^3/3 - x$ , and

$$h(x) = \begin{cases} -x^2 - 0.25, & \text{for } |x| < 0.5 \\ -x, & \text{for } x > 0.5 \\ x, & \text{for } x < -0.5. \end{cases}$$

$x_2$  and  $x_4$  represent the action potentials of the SA and AV nodes respectively. The interaction between the SA and AV nodes is modeled as two coupled

nonlinear oscillators, associated with an equivalent electronic circuit depicted in Fig. 1. To simulate the heartbeat dynamics, Eqs. (1-4) were solved using the fourth order Runge-Kutta algorithm with step size  $h = 0.001$ .

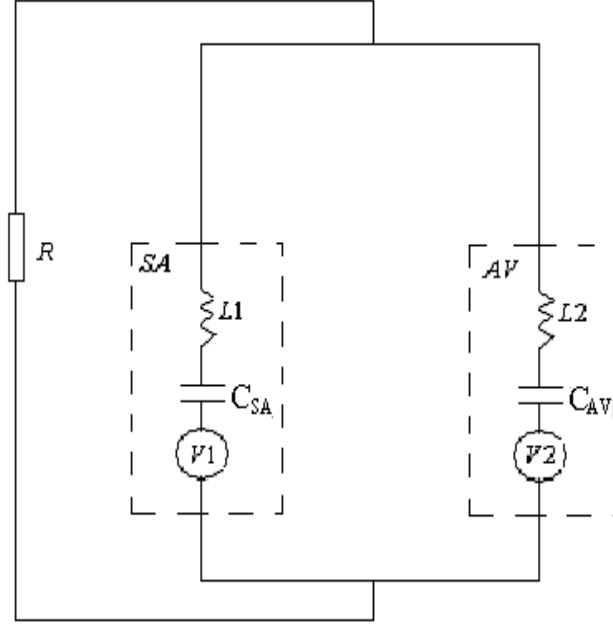


**Fig. 1.** Equivalent electrical circuit describing the model constituted by two coupled nonlinear oscillators representing the SA and AV nodes.

### 3 Control Method and Results

#### 3.1 Continuous control

In normal sinus rhythm dynamics, the SA and AV nodes are approximately 1:1 phase locked. That is, every time the SA node depolarizes, there is one AV node depolarization. In various arrhythmias, different phase locking (n:m) behaviors occur. Our aim is to use feedback control to resynchronize the depolarization of the SA and AV nodes. That is, to make it 1:1 phase locked again using a gentle control or coaxing strategy (by applying low intensity

stimuli to the system). Since an arrhythmia is related to the asynchrony between the SA and AV oscillators, we utilize the difference in heartbeat period between the SA and AV node oscillations as a feedback control signal. The goal is to induce the faster oscillator to run slower and the slow oscillator to run faster. According to [1], the frequency of the SA (AV) beat is proportional to  $\frac{1}{C_{SA}}$  ( $\frac{1}{C_{AV}}$ ). We thus introduce an (external) control capacitor  $C$  whose inverse is updated recursively as

$$\left(\frac{1}{C}\right)_i = \left(\frac{1}{C}\right)_{i-1} + k(T_{AV} - T_{SA})_i \quad \text{for } i = 1, 2, 3, \dots, \quad (5)$$

where  $T_{AV}$  ( $T_{SA}$ ) is the period between two successive AV (SA) beats,  $k$  is a simple gain factor,  $i$  is an index for the number of times  $T_{AV}$  and  $T_{SA}$  are updated.

The controlled model is as follows:

$$\dot{x}_1 = \frac{1}{C_{SA}} x_2 - \frac{1}{C} x_2, \quad (6)$$

$$\dot{x}_2 = -\frac{1}{L_{SA}} [x_1 + g(x_2) + R(x_2 + x_4)], \quad (7)$$

$$\dot{x}_3 = \frac{1}{C_{AV}} x_4 + \frac{1}{C} x_4, \quad (8)$$

$$\dot{x}_4 = -\frac{1}{L_{AV}} [x_3 + f(x_4) + R(x_2 + x_4)], \quad (9)$$

with  $1/C$  calculated using the recursive relation given in Eq. (5). Figure 2 is the equivalent electrical circuit of the system with control. The general idea is that if the SA node runs faster than the AV node, then  $(T_{AV} - T_{SA}) > 0$ , which will increase the value of  $1/C$  from Eq. (5). According to Eqs. (6) and (8), this will cause the SA node to run slower and the AV node faster. The negative feedback of frequency difference is thus realized. Initially,  $1/C$  should be set to zero, and then should be self-modified by the feedback error on each iteration until a point in time when the alternating pattern halts and sinus rhythm is restored. The adjustment will not stop as long as the frequency difference remains. In an actual pacemaker implementation one would need to (and would only be able to) speed up the slower node (AV node) in order to keep pace with the faster one (SA node). Therefore the control stimulus would be applied only to the AV node using Eq. (8) and not to the SA node. In the results that follow then, we used Eqs. (1, 5, 7-9) only (and not Eq. (6)) to simulate control of the system.

The values of  $T_{AV}$  and  $T_{SA}$  are obtained by measuring the time interval between two successive peaks of the waveforms of the AV and SA nodes, respectively. A peak is determined to have occurred if the signal increased through a threshold, passed over a local maximum and then decreased through another threshold.

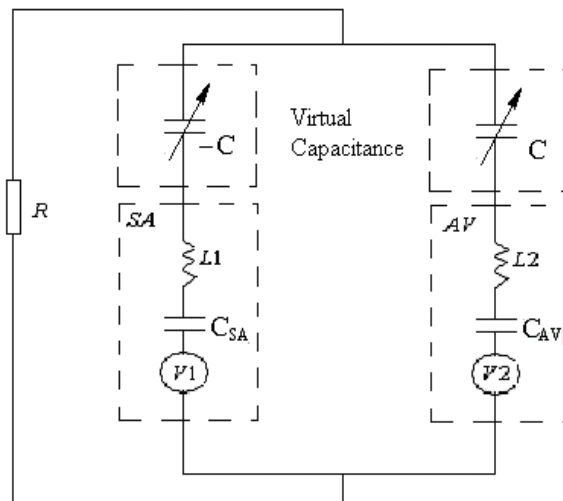


**Fig. 2.** Equivalent electrical circuit for the controlled system.

The value of  $k$  can be chosen between 1 and 10 with little difference in performance. The larger  $k$  is, the faster synchronization is achieved. Normal heartbeat dynamics can be obtained with

$$C_{SA} = 0.25, L_{SA} = 0.05, C_{AV} = 0.675, L_{AV} = 0.027, R = 0.11. \quad (10)$$

By varying the coupling resistance  $R$  while keeping other parameters the same as Eq. (10), we obtain one type of arrhythmia known as  $2^\circ$  AV block of the Wenckebach type. It is usual to describe this arrhythmia with two integers  $n : m$ , which means the atria contract  $n$  times while the ventricles  $m$  times. Figure 3(a) shows both the uncontrolled and controlled 3:2 Wenckebach rhythm with  $R = 0.018$ . The controller is turned on at time 5 and turned off at time 15, with the control gain  $k = 2$ . By varying  $C_{SA}$  while keeping other parameters the same as Eq. (10), we obtain another type of arrhythmia known as  $n : 1$  AV block. Figure 3(b) shows both the uncontrolled and controlled 3:1 AV block with  $C_{SA} = 0.10$ . The controller is turned on at time 5 and turned off at time 10, using the control gain  $k = 2$ .

Figure 4(a) is analogous to Fig. 3(a) with the exception that zero-mean Gaussian white noise has been added to both  $x_2$  and  $x_4$ . The root-mean-square (RMS) amplitude of the white noise ( $\sigma$ ) is 0.04 and 0.06, respectively. Similarly, Fig. 4(b) is the “noisy” version of Fig. 4(a) with  $\sigma = 0.1$  for both  $x_2$  and  $x_4$ .

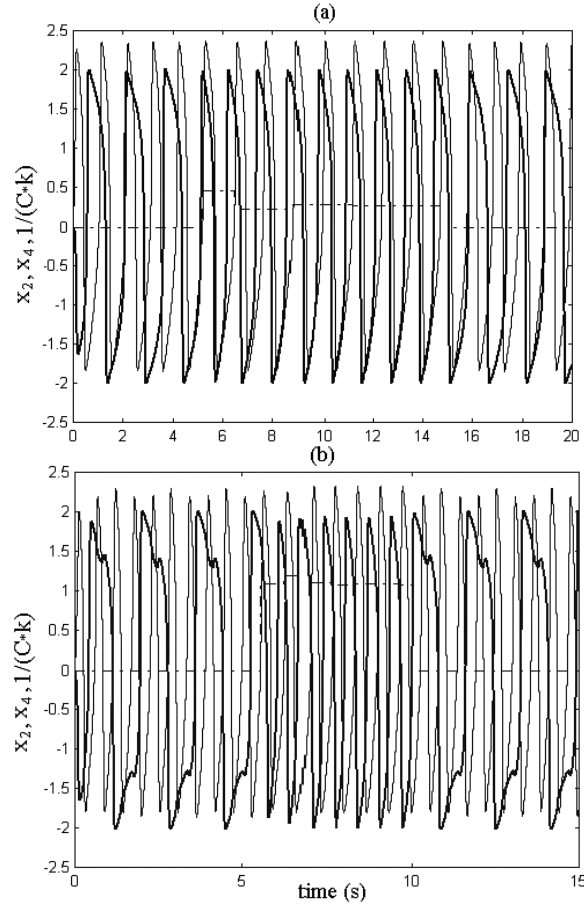


**Fig. 3.** (a) 3:2 Wenckebach rhythm with  $R = 0.018$ ,  $k = 2$ . The controller is turned on at time 5 and turned off at time 15. The thin line is for the SA node, the thick line is for the AV node, the dotted line is the control signal. (b) 3:1 AV block.  $C_{SA} = 0.10$ ,  $k = 2$ . The controller is turned on at time 5 and turned off at time 10. The thin line is for the SA node, the thick line is for the AV node, the dotted line is the control signal ( $1/C$ ) scaled by  $1/k$  for plotting purposes.

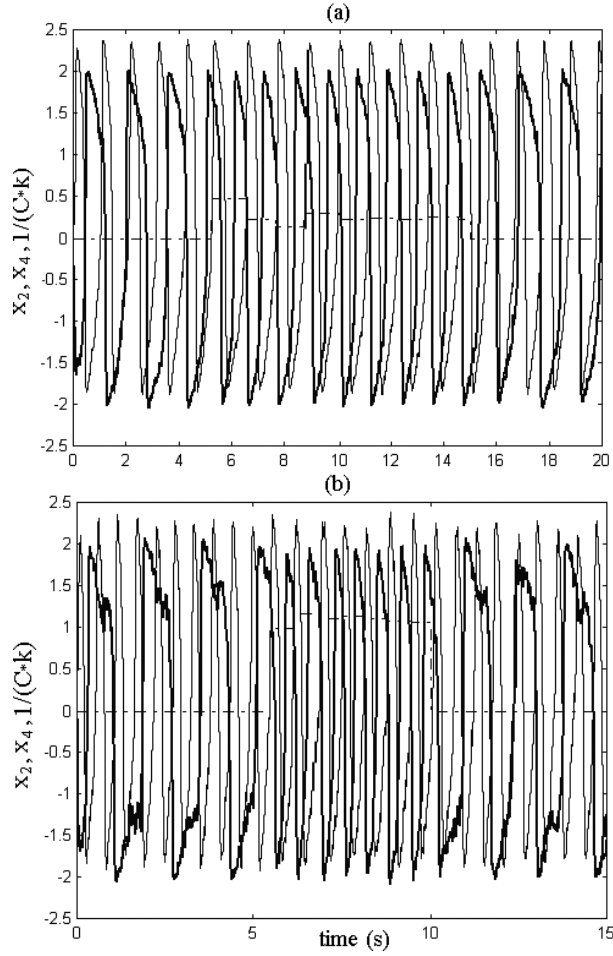


**Fig. 4.** (a) 3:2 Wenckebach rhythm with  $R = 0.018$ ,  $k = 4$ ,  $\sigma_{SA} = 0.04$ , and  $\sigma_{AV} = 0.06$ . The controller is turned on at time 5 and turned off at time 15. The thin line is for the SA node, the thick line is for the AV node, the dotted line is the control signal. (b) 3:1 AV block.  $C_{SA} = 0.10$ ,  $k = 2$ ,  $\sigma_{SA} = \sigma_{AV} = 0.1$ . The controller is turned on at time 5 and turned off at time 10. The thin line is for the SA node, the thick line is for the AV node, the dotted line is the control signal ( $1/C$ ) scaled by  $1/k$  for plotting purposes.

### 3.2 Discrete control

In an actual cardiac preparation, control is not normally applied continuously as above. Instead, electrical stimulations are delivered discretely and periodically. From Eq. (8) one sees that the final effect of the control in every time step is to change  $x_4$  to  $(1 + \frac{C_{AV}}{C})x_4$ , which is derived from

$$\frac{1}{C_{AV}} x_4' = \left( \frac{1}{C_{AV}} + \frac{1}{C} \right) x_4, \quad \rightarrow \quad x_4' = \left( 1 + \frac{C_{AV}}{C} \right) x_4.$$

To this end, we shall apply a stimulation with strength  $E$  proportional to

$$(x_4' - x_4) = \left( \frac{C_{AV}}{C} \right) x_4$$

at every time step  $i\tau$

$$E(i\tau) \propto \frac{x_4(i\tau)}{C(i\tau)} \quad \text{for } i = 1, 2, 3, \dots \quad (11)$$

The constant  $\tau$  is the time interval between two successive electrical stimulations. Note that any uncertainties are included in the gain factor  $k$  (Eq. (5)), thus we can turn Eq. (11) into an equality

$$E(i\tau) = \frac{x_4(i\tau)}{C(i\tau)} \quad \text{for } i = 1, 2, 3, \dots \quad (12)$$

The discrete and the continuous controls are identical if  $\tau$  is chosen to be the same as the step size of the Runge-Kutta algorithm. As  $\tau$  increases, the ability to control the system slowly degrades. However, according to our simulations it can still perform well with  $\tau$  as large as 0.15. The control is ineffective with  $\tau$  greater than 0.2. There are several merits of the control strategy Eq. (12). First, it can be applied directly without any knowledge of the model (even though it is derived from the model). This is an advantage as compared with some methods presented in [7, 8]. Second, the algorithm is quite simple. One needs only to detect the value of the AV action potential  $x_4$  at constant time intervals  $\tau$ . The control gain  $k$  can be chosen over a large range with no essential performance difference. Finally, only one parameter  $k$  needs to be adjusted, which is easier as compared with the OGY method. In simulations, the discrete control is realized by altering the action potential of the AV node from  $x_4$  to  $x_4'$  at every time interval  $\tau$ . In an actual pacing system discrete electrical stimuli would be applied through an electrode placed near the AV node so as to alter its action potential from  $x_4$  to  $x_4'$  at every time interval  $\tau$ . Figure 5 shows both the uncontrolled and controlled 2:1 AV block with  $C_{SA} = 0.15$ . The controller is turned on at time 5 and turned off at time 20, with  $\tau = 0.1$  and  $k = 8$ .

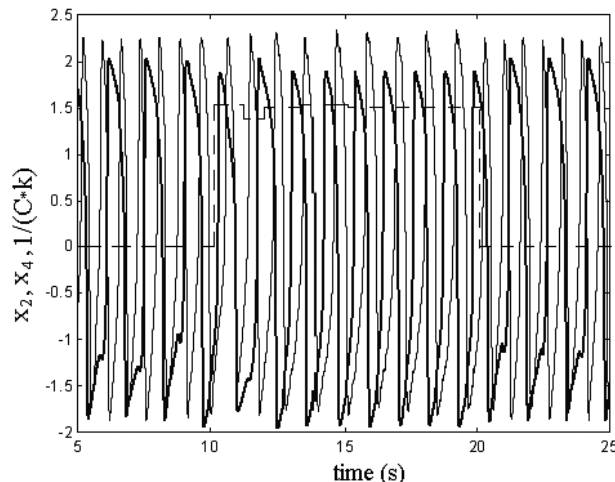


**Fig. 5.** Discrete control.  $C_{SA} = 0.15$  (2:1 AV block),  $\tau = 0.1$ ,  $k = 8$ . The controller is turned on at time 5 and turned off at time 20. The thin line is for the SA node, the thick line is for the AV node, the dotted line is the control signal ( $1/C$ ) scaled by  $1/k$  for plotting purposes (the control signal appears continuous in the plot due to the small  $\tau$  used).

## 4 Conclusions

We have presented a simple control method for stabilizing some pathological behaviors of a nonlinear heartbeat model with and without random noise. Comparison of this control method with others (particularly the OGY method) has been discussed. The continuous controller was discretized to demonstrate that it is algorithmically realizable within a digital pacemaking device design by using an external control capacitor  $C$  that discharges its energy through a stimulating electrode. This electrode would normally be placed near the AV node in order to speed up its rate to keep pace with the faster SA node. The control algorithm should be able to be implemented in an actual pacing environment at least in the same manner as those of Garfinkel *et al.* [1], Hall *et al.* [13], and Christini *et al.* [14]. As mentioned in the introduction, the control algorithm proposed here might eliminate the need for a timing reel thereby rendering it magnet-safe. This would allow the pacemaker to be used when patients must undergo an MRI scan. The present algorithm does not address the conditions of sinus arrest/prolonged sinus pause and complete atrioventricular block without escape rhythm. However, these problems may be correctable using alternative or adjunctive algorithmic approaches which are beyond the scope of the present chapter.

## References

1. Garfinkel A., Spano M. L., Ditto W. L., Weiss J. N. (1992) Controlling cardiac chaos. *Science*, **257**, 1230–1235.
2. Ott E., Grebogi C., Yorke J. A. (1990) Controlling chaos. *Phys. Rev. Lett.*, **64**, 1196–1199.
3. Van Der Pol M. (1928) The heart-beat considered as a relaxation oscillation and an electrical model of the heart. *Phil. Mag.*, **6**, 763–775.
4. West B. J., Goldberger A. L. (1985) Nonlinear dynamics of the heartbeat. The AV junction: Passive conduit or active oscillator? *Physica D*, **7**, 198–206.
5. Signorini M. G., Cerutti S. (1998) Simulation of Heartbeat Dynamics: A Nonlinear Model. *Int. J. Bifurc. Chaos*, **8**, 1725–1731.
6. Di Bernardo D., Signorini M. G., Cerutti S. (1998) A Model of Two Nonlinear Coupled Oscillators for The Study of Heartbeat Dynamics. *Int. J. Bifurc. Chaos*, **8**, 1975–1985.
7. Brandt M. E., Chen G. (1996) Feedback control of a quadratic map model of cardiac chaos. *Int. J. Bifurc. Chaos*, **6**, 715–723.
8. Glass L., Zeng W. (1994) Bifurcations in flat-topped maps and the control of cardiac chaos, *Int. J. Bifurc. Chaos*, **4**, 1061–1067.
9. Brandt M. E., Chen G. (1996) Controlling the dynamical behavior of a circle map model of the human heart. *Biol. Cybern.*, **74**, 1–8.
10. Brandt M. E., Shih H. T., Chen G. (1997) Linear time-delay feedback control of a pathological rhythm in a cardiac conduction model. *Phys. Rev. E*, **56**, R1334–1337.
11. Brandt M. E., Chen G. (1997) Bifurcation control of two nonlinear models of cardiac activity. *IEEE Trans. Circ. Sys. I*, **44**, 1–4.
12. Brandt M. E., Chen G. (2000) Delay feedback control of cardiac activity models. In: G. Chen (ed.) *Controlling Chaos and Bifurcations in Engineering Systems*, pp. 325–345. Boca Raton: CRC Press.
13. Hall K., Christini D. J., Tremblay M., Collins J. J., Glass L., Billette J. (1997) Dynamic control of cardiac alternans. *Phys. Rev. Lett.*, **78**, 4518–4521.
14. Christini D. J., Stein K. M., Markowitz S. M., et al. (2001) Nonlinear-dynamical arrhythmia control in humans. *Proc. Nat. Acad. Sci.*, **98**, 5827–5832.